Sensors & Transducers, Vol. 174, Issue 7, July 2014, pp. 240-245

Sensors & Transducers

Optimization of Axial Resolution in Ultrasound Elastography

Zhihong Zhang, Haoling Liu, Congyao Zhang, D. C. Liu
School of Computer Science, Sichuan University, Chengdu 610065, China
Tel.: +28-731-15399907889
E-mail: z.zhihong85@gmail.com

Received: 13 March 2014 /Accepted: 30 June 2014 /Published: 31 July 2014

Abstract: To improve the axial resolution of ultrasonic elastography, by taking the advantage of code excitation and frequency compounding, multi-frequency with coded excitation for elastography (FCCE) was proposed. FCCE adopts the Chirp signal excitation scheme and strikes a balance in the selection of sub-signal bandwidth, the bandwidth overlap and the number of sub-strain image based on theoretical derivation, so as to further improve the axial resolution of elastic image. On MATLAB, multi-frequency with coded excitation for elastography was implemented and compared with short pulse. Experiments have proved that, compared with the short pulse, the elastographic signal-to-noise ratio (*SNRe*) and contrast-to-noise ratio (*CNRe*) were improved significantly. Moreover, probing depth, axial resolution and target detection were improved too. Therefore, the FCCE technology can effectively improve the elastography quality and can be applied to ultrasonic clinical trials. *Copyright © 2014 IFSA Publishing, S. L.*

Keywords: Ultrasonic elastography, Axial resolution, Coded excitation, Multi-frequency compounding L.

1. Introduction

Elastography, the imaging modality of elastic properties of biological tissue using ultrasound, was firstly presented by A. Hassen in 1991 [1]. In general, a small external mechanical pressure is applied on soft tissue. Axial strain calculation compares the signal before the application of force, or pre-compression signal, with the post-compression signal. Elastogram is calculated as the gradient of the axial displacements and displayed as a gray scale image where the dark areas correspond to hard tissue while the light areas indicate soft tissue. With ultrasonic elastography, elastic properties are measured quantitatively, which offers more information than qualitative analysis of palpation.

In 2011, transmit-side frequency compounding elasticity imaging technique (TSFC) was proposed in B. Park [2]. Simulation data and anthropomorphic phantom data demonstrate that TSFC can effectively eliminate amplitude modulation noise and improve elastographic signal-to-noise ratio (*SNRe*) and elastographic contrast to noise ratio (*CNRe*) of ultrasound elastic strain imaging. In 2005, coed excitation for ultrasound elatography was introduced for the first time in J. W. Goodman [3]. It pointed out that coded excitation can effectively suppress the noise of decorrelation in ultrasound elastography when the system SNR is low. In 2012, 5 coded excitation solutions based on Chirp signals were proposed and applied in ultrasound elastography in C. B. Burckhardt [4]. Based on the research on transmit-side multi-frequency compounding (FC) and coded excitation (CE), it can be said that the combination of these two technologies and their applications in elastography are very promising.

2. Method

2.1. Theoretical Background

From the combination of principles and processes of noise suppression, TSFC can act as the right assistive technology for CE. Based on above theoretical study, transmit-side multi-frequency coded excitation compounding technology (*FCCE*) is proposed. By carrying out weighted compounding on sub strain images excited by coded signals with different center frequencies and utilizing the decorrelation of strain noise, the strain noise and the noise introduced by coded excitation can be further suppressed. Finally, the image quality is improved with the advantage of increased detecting depth and enhanced strain detection capability. For TSFC technology, the greater the decorrelation of signals is, the further will noise be eliminated after weighted average while useful information is protected. Therefore, for compounding technology, the smaller the cross-correlation of two signals is, the better noise-elimination capability it has.

Theoretically, the *SNRe* of sub strain images after compounding can be expressed as:

$$SNRe = \frac{E\left(\overline{X}\right)}{\sqrt{Var\left(\overline{X}\right)}} = \sqrt{\frac{N}{1+(N-1)\rho}} \times \frac{\mu}{\sigma}, \quad (1)$$

where N is the number of sub strain images. μ and σ are, respectively, the mean and standard deviation of the strain estimates in a region of uniform elasticity. ρ is the normalized cross-correlation coefficient of sub-strain images. Suppose that A and B are two sub strain images with the size of m×n obtained by sending two ultrasound with different center frequencies, then ρ can be expressed as:

$$\rho = \frac{\sum_{i=1}^{m}\sum_{j=1}^{n}(A_{i,j}-\overline{A})(B_{i,j}-\overline{B})}{\sqrt{\sum_{i=1}^{m}\sum_{j=1}^{n}(A_{i,j}-\overline{A})^2 \sum_{i=1}^{m}\sum_{j=1}^{n}(B_{i,j}-\overline{B})^2}}, \quad (2)$$

The following conclusions can be derived from Eqs. 1 and 2:

1) When sub strain images are completely decorrelated, i.e. ρ=0, the *SNRe* of elastic strain images after compounding will be improved by a factor of $\sqrt{N}$;

2) When sub strain images are completely correlated, i.e. ρ=1, the *SNRe* after compounding remains unchanged;

3) When sub strain images are partially correlated, i.e. 0<ρ<1, the *SNRe* after compounding will be improved by a factor of $\sqrt{N/\left(1+(N-1)\rho\right)}$.

It can be seen that the smaller the normalized cross-correlation coefficient ρ of sub strain images is, the more improvement TSFC will bring to image quality. And if the respective ρ of sub images is of same value, then the more sub images there are, the better *SNRe* is. However, it can be derived from Eq. 1, if *SNRe* of compounding result of K+1 sub strain images is higher than that of K sub strain images, then the following equation must hold:

$$\rho_{K+1} < \frac{1}{K^2}\left[\frac{SNRe_{K+1}}{SNRe_K}(K+1) + \frac{SNRe_{K+1}}{SNRe_K}(K^2-1)\rho_K - K\right], \quad (1)$$

where ρ_N are the cross-correlation coefficients of N sub strain images, $SNRe_N$ is the average *SNRe* of N sub strain images. From last formula, ρ_{K+1} is affected mainly by ρ_K, K and $SNRe_{K+1}/SNRe_K$. So there are many factors affecting the imaging results, and the increase of the number of sub strain images cannot guarantee that ρ remain unchanged. Therefore, the number of sub strain images is not the sole determining factor.

Cramer-Rao lower bound was proposed and the theoretical minimum variance of displacement distribution σ^2_{CRLB} was provided [4], as shown in Eq. 4.

$$\sigma^2_{CRLB} \cong \frac{3}{2\pi^2 T\left(B^3+12Bf_0^2\right)}\left[\frac{1}{\rho'}\left(1+\frac{1}{SNRs^2}\right)^2 - 1\right], \quad (4)$$

where T is the duration time of the signal, B is the bandwidth, f_0 is the center frequency of the probe, ρ' is the cross-correlation coefficient of two frame signals before and after compression, *SNRs* is the signal-to-noise of the system. One of CE's characteristics is that the long coded signals with big bandwidth to excite probes can be sent. As can be seen from Eq. 4, theoretically the longer the coded signal sustains and the bigger the bandwidth is, the better the imaging effect is. Due to the beam synthesis and imaging safety, the length of the encoded signal actually requires an appropriate range, while the coded bandwidth is affected by the probe bandwidth. Therefore, the cross-correlation coefficient ρ of bandwidth B and sub-strain image becomes the most important balance point of the combination of CE and TSFC. The introduction of TSFC into CE requires coded signals with different center frequencies to excite probes. At this point, in addition to the bandwidth of the probes, the coded signal bandwidth can be limited by the bandwidth overlaps of multi frame coded signals. This is because that the higher the bandwidth overlaps are, the higher the cross-correlation coefficient ρ of sub strain images is. then TSFC cannot effectively eliminate noise through compounding. If the bandwidth of coded signal was reduced recklessly to make the cross-correlation coefficient ρ smaller, the effect of CE technology will be affected, weakening its ability of increasing detecting depth and improving target detection, and the ability to fight against attenuation. Therefore, tradeoffs need to be made when selecting the sub-signal bandwidth,

bandwidth overlap and the number of sub strain images.

2.2. Technical Principles and Processes

Coded signals with different center frequencies are used to excite probes in *FCCE*. Then the sub strain images are obtained by displacement and strain estimation. Finally, compounding strain images are obtained through weighted compounding to improve detecting depth, detecting capability, *SNRe* and *CNRe*. Every sub strain image is obtained through coded excitation and has higher *SNRe*. Smaller displacement estimation signal window can be used to get better resolution. Therefore, the quality starting point of compounding images is higher.

Strain images excited by Chirp signal, 13-bit Barker code, 32-bit Suboptimal code and 32-bit Golay code were compared through experiments respectively in J.W. Goodman [3]. Under different eSNR and attenuation coefficients, best imaging results and best robustness were obtained by Chirp code and Golay code excitations. While when adopting *FCCE* technology, it needs transmit multi-frame signals during the movement of tissues, but the movement among tissues will weaken the sidelobe suppression capability of Golay code. In conclusion, Chirp linear frequency modulation signal is employed as the coded signal in this paper.

The process of *FCCE* is shown in Fig. 1.

Step 1: Set coded signals as excitation signal for probes, such as Chirp code and Barker code. And configure the center frequency ($f_1, f_2, \ldots, f_N$), bandwidth, pulse duration, amplitude suppressing window function of the signal sequences and excitation sequence (center frequency): $f_1, f_2, \ldots, f_N$, $f_1, f_2, \ldots, f_N$.;

Step 2: The probe was used to compress tissues and was controlled to send 2N ultrasound signals with N different center frequencies alternatively;

Step 3: Carry out pulse compression on echoes after receiving 2N frames of echo sequences;

Step 4: Establish N echo buffer queues $\{q_j\ (j=1,2,\ldots,N)\}$. q_j will store the echo signals of center frequency f_i (i=1,2,…, N) and echo signals will be classified according to center frequency;

Step 5: Utilizing two signal frame in each echo buffer queue $\{q_j\ (j=1,2,\ldots,N)\}$, sub strain image queue$\{s_i\ (i=1,2,\ldots,N)\}$ is obtained through displacement estimation and strain estimation;

Step 6: Weighted compounding: Use a weighted compounding method to combine N sub strain images into one strain image:

$$FC(N)=\frac{\sum_{i=1}^{N}\alpha_i X(f_i)}{\sum_{i=1}^{N}\alpha_i}, \quad (5)$$

where N is the number of sub strain images, α_i is the weight of ith sub strain image, $X(f_i)$ is the sub strain image with center frequency of f_i. If using averaging method, then α_i =1/N (i=1, 2, …, N).

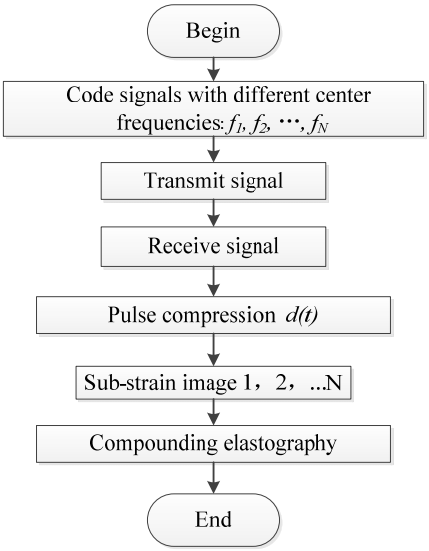

Fig. 1. Flow chart of FCCE technology.

3. Experimental Step

RF data of each frame were simulated using Field II [5]. The 1st uniform phantom consists of 3 × 105 scatterers (fully developed) distributed uniformly throughout 100 mm × 30 mm × 10 mm volumes with scattering strengths Gaussian distributed. The ideal strain image of the phantom is shown in Fig. 2 (a), while the modular ratio is 3.2. The second uniform phantom consists of 2 × 105 scatterers (fully developed) distributed uniformly throughout 50 mm × 40 mm × 10 mm volumes with scattering strengths Gaussian distributed. The ideal strain image of the phantom is shown in Fig. 2 while the modular ratio is 0.5. Transducer parameters and processing parameters in experiments are shown in Table 1.

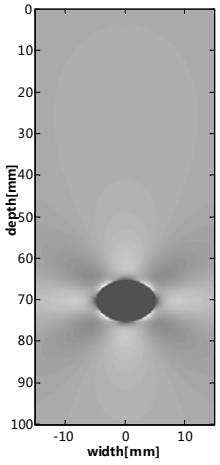

Fig. 2 (a). Ideal strain diagram software organization simulation motion model. No.1 Body model spherical hard lesion.

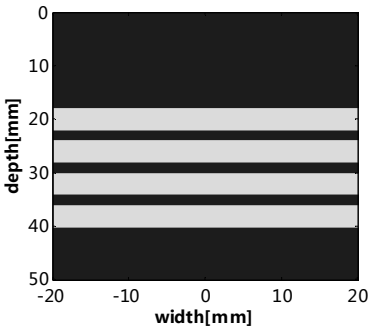

Fig. 2 (b). Ideal strain diagram software organization simulation motion model. No. 2 Body model: 4 horizontal stripe soft lesions.

Table 1. Default values for the simulation parameter study.

Parameters	$U_{m,}$ (V)	$I_{s,}$ (mA)
RF Sampling frequency	f_s	100 MHz
Pitch of transducer element	ω	0.208 mm
Height of transducer element	h_e	5 mm
kerf	*Ke*	0.035 mm
Number of elements	*N*	192
Number of active elements	N_a	64
Transmit apodization	A_{xmt}	hamming
Receive apodization	A_{rec}	hamming
Focus	*Z*	30 mm
Assumed speed of sound	*C*	1540 m/s
Elevation focus	R_e	20 mm
Modular ratio of Phantom	N0.1	3.2
	N0.2	0.5
Attenuation coefficient	ρ	0.5 dB/cm/MHZ
Echo signal-to-noise ratio	eSNR	50 dB

Experiment 1 chooses the first simulation body model (containing hard spherical lesion) and test the strain signal to noise ratio *SNRe* and contrast to noise ratio *CNRe* of resulting image.

Experiment 2 chooses No. 2 simulation body model for imaging and calculates the strain signal to noise ratio *SNRe* and *CNRe* contrast to noise ratio of resulting image.

3. Experiment Results and Discussions

3.1. Experiment 1

Fig 3 (a) and Fig. 3 (b) show the experimental resulting image of short pulse and *FCCE* while the attenuation coefficient is 0.7 dB/cm/MHz and eSNR is 50 dB. Fig. 3 (c) and Fig. 3 (d) show the ROI (the depth of 70 mm-100 mm) details of Fig. 3 (a) and Fig. 3 (b). It can be seen that the calculation errors appear noticeably in short pulse image in the deeper area. At the depth of 70 mm, lesions are almost submerged by strain noise, and the edge is obfuscated. In *FCCE* image, by contrast, noise nearby the lesions is less. The lesions' edge is clear and the shape is complete, although there are slight calculation errors when the depth is greater than 90 mm.

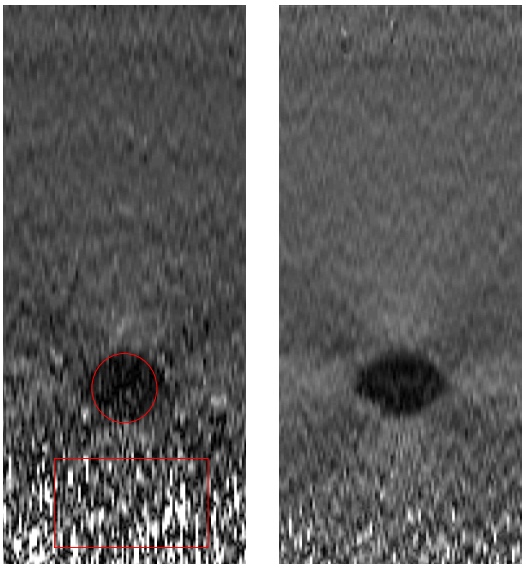

(a) short pulse
SNRe =3.28
CNRe =3.89

(b) *FCCE*
SNRe =6.08
CNRe =18.40

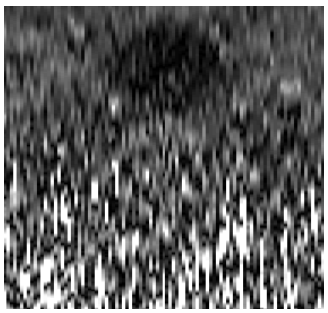

(c) short pulse detail (70 *mm*-100 *mm*)

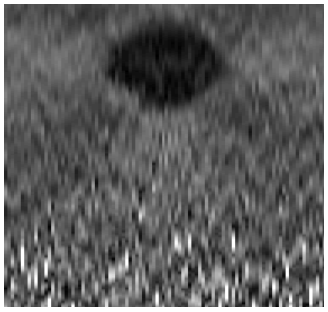

(d) *FCCE* detail (70 *mm*-100 *mm*)

Fig. 3 Attenuation coefficient is 0.7 dB/cm/MHz, experimental resulting image of short pulse and *FCCE* with details.

Fig. 4 shows the longitudinal strain values in the middle area of the short pulse and *FCCE* strain images in Fig. 3. In the healthy background tissue when the depth is below 65 mm, the disturbance of *FCCE* strain value is less severe than that of short pulse, however, the difference is insignificant. When the depth is between 65 mm and 75 mm in internal hard lesion, the disturbance of *FCCE* strain value is less violent than that of short pulse, which shows the disturbance of *FCCE* strain value is relatively even in lesion parts. When the depth is above 75 mm, the disturbance of short pulse strain value is severe, which represents that the depth is beyond the effective detection range of short pulses. Besides, although the disturbance of *FCCE* goes up as depth grows, the variation is relatively stable which indicates that it is still within the detection depth.

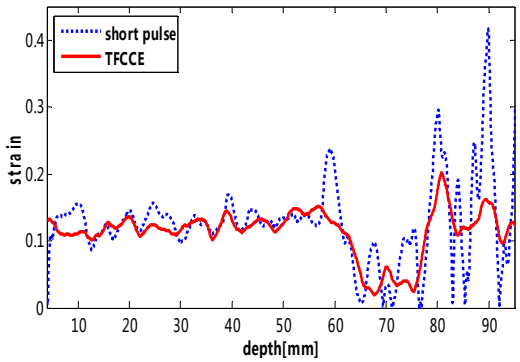

Fig. 4. Attenuation coefficient is 0.7 dB/cm/MHz, longitudinal strain values in the middle location of the short pulse and *FCCE*.

From the above analysis, under the condition of different attenuation coefficient, *FCCE* can improve both the image's *SNRe* and *CNRe*.

Especially in high tissue attenuation, short pulse is unable to guarantee the basic quality of the image, while *FCCE* can help to get a strain image with medium quality.

3.2. Experiment 2

The contrast strain images in this experiment are mainly from the following two types of simulation. 1) Regular short pulse (two cycles Gaussian modulation cosine signal) with center frequency of 5 MHZ. 2) The results of *FCCE* process.

In Fig. 5 (a) – Fig. 5 (d), attenuation coefficient is 0.4 dB/cm/MHz, and eSNR is 30 dB. Figs.5 (a), 5 (b) and Fig. 5 (c) respectively show the strain image of short pulse process when the displacement of the estimated signal window length is 20, 30, 40 pixels. Fig. 5 (d) shows the strain image of *FCCE* process when the displacement of the estimated signal window length is 20 pixels.

The calculated of ROI in the red box in Fig. 5 are 4.83, 5.86, 8.68 and 8.70. Fig. 5 (a) and Fig. 5 (d) show that the longitudinal resolution of strain image is close when the displacement of the estimated signal window length is 20 pixels. Fig. 5 (c) and Fig. 5(d) show that the *SNRe* obtained by the short pulse whose window length is 40 pixels is close to the one obtained by *FCCE* whose window length is 20 pixels.

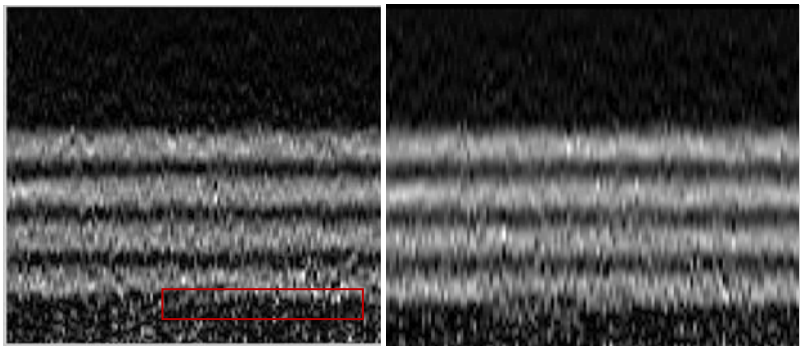

(a) short pulse, *W*=20 *pt; SNRe* =4.83

(b) short pulse, W=30 pt; *SNRe*=5.86

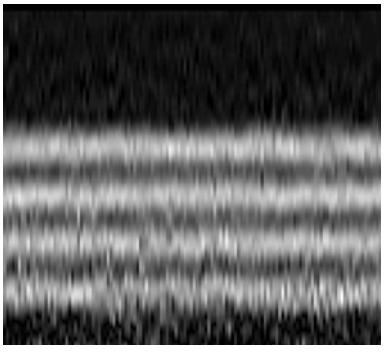

(c) short pulse, W=40 pt; *SNRe* =8.68

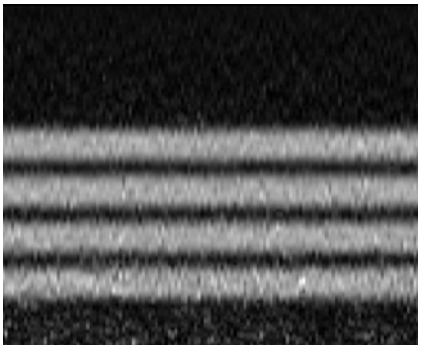

(d) *FCCE*, W=20 pt; *SNRe* =8.70

Fig. 5. The resulting image of short pulse and *FCCE* with different displacement estimation window.

Fig. 6 shows the longitudinal strain values in the middle location of the strain images of short pulse whose window length is 40 pixels and *FCCE* whose window length is 20 pixels.

The horizontal arrow marks the interval width among soft white lesions. This approach can visually help us to analyze the effects of short pulse and *FCCE* on the longitudinal resolution.

The interval widths among lesions of short pulse image are all wider than those of *FCCE* image, indicating that the longitudinal resolution of *FCCE* is better, which also can be seen in Fig. 5(a) and Fig. 5(b).

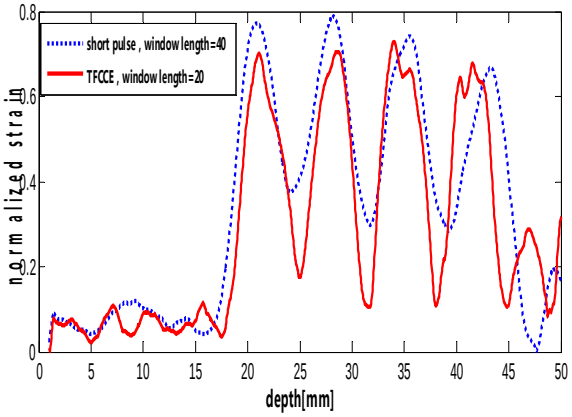

Fig. 6. Longitudinal strain values in the middle location of the strain images of short pulse with window length of 40 and *FCCE* with window length of 20.

Based on the analysis above, we can get the following conclusions: *FCCE* can use a shorter displacement estimation of signal window than short pulse in the case of the same noise level, which indicates that *FCCE* has a potential for increasing longitudinal resolution of the strain image.

5. Conclusions

The coded excitation and frequency compounding in ultrasound elastography was discussed. The academic background and the advantage of coded excitation and Transmit-side Frequency Compounding were introduced. An ultrasound elasticity imaging improvement technique based on coded excitation and Transmit-side Frequency Compounding technology naming Transmit side multi-Frequency Compounding with Coded Excitation for Elastography (*FCCE*) was proposed. Re-SN decreases with increasing attenuation coefficient. *SNRe* and *CNRe* of *FCCE* increase by 85 % and 373 % than those of short pulse when the attenuation coefficient is 0.7 dB/(cm·MHz). The lesion at 70 mm is almost overwhelmed by the strain noise and its edge is not clear, while in the results of *FCCE*, the lesion is complete and its edge is clear although there is slight miscalculation at the depth of 90 mm. The impact of *FCCE* on resolution has also been analyzed. Probing depth, axial resolution and target detection were improved too. Based on experimental data analysis, we can come to the conclusion that the use of *FCCE* can improve the quality of ultrasound elastography.

Reference

[1]. A. Hassen, Predicting percentage of intramuscular fat using two types of real-time ultrasound equipment, *Journal of Animal Science*, Vol. 79, Issue 1, 2000, pp. 11-18.

[2]. B. Park, Measuring intramuscular fat in beef with ultrasonic frequency analysis, *Journal of Animal Science*, Vol. 72, Issue 3, 1994, pp. 117-125.

[3]. J. W. Goodman, Some fundamental properties of speckle, *Journal of the Optical Society of America,* Vol. 66, No. 6, 1976, pp. 1145-1150.

[4]. C. B. Burckhardt, Speckle in ultrasound B-Mode scans, *IEEE Transactions on Sonics and Ultrasonics*, Vol. 25, Issue 8, 1978, pp. 1-6.